Hyperphosphorylation of Tau Induces Local Polyproline II Helix†

Agata A. Bielska and Neal J. Zondlo*

Department of Chemistry and Biochemistry, University of Delaware, Newark, Delaware 19716

Received December 31, 2005; Revised Manuscript Received February 27, 2006

ABSTRACT: Alzheimer's disease is characterized by two protein precipitates, extracellular amyloid plaques and intracellular neurofibrillary tangles (NFTs). The primary constituent of NFTs is a hyperphosphorylated form of the microtubule-binding protein tau. Hyperphosphorylation of tau on over 30 residues, primarily within proline-rich sequences, is associated with conformational changes whose nature is poorly defined. Peptides derived from the proline-rich region of tau (residues 174−242) were synthesized, and the conformations were analyzed for the nonphosphorylated and phosphorylated peptides. CD and NMR data indicate that phosphorylation of serine and threonine residues in proline-rich sequences induces a conformational change to a type II polyproline helix. The largest phosphorylation-dependent conformational changes observed by CD were for tau peptides incorporating residues 174−183 or residues 229−238. Phosphoserine and phosphothreonine residues exhibited ordered values of $^3J_{\alpha N}$ (3.1−6.2 Hz; mean = 4.7 Hz) compared to nonphosphorylated serine and threonine. Phosphorylation of a tau peptide consisting of tau residues 196−209 resulted in the disruption of a nascent α-helix. These results suggest that global reorganization of tau may occur upon hyperphosphorylation of proline-rich sequences in tau.

Alzheimer's disease is a neurological disorder characterized by protein misfolding. Two distinct protein aggregates are observed, extracellular amyloid plaques and intracellular neurofibrillary tangles (NFTs[1]). Neurofibrillary tangles consist primarily of hyperphoshphorylated tau protein as well as other microtubule-associated proteins (MAPs) (*1*−*6*). Under normal cellular conditions, tau binds to microtubules in neurons and stabilizes their elongated structure in the axon. In diseased cells, tau becomes hyperphosphorylated. Hyperphosphorylation of tau has been proposed to induce a conformational change in the protein that causes tau to aggregate and precipitate as NFTs. The mechanisms associating hyperphosphorylated tau and Alzheimer's disease pathology are a subject of active research. A gain of function mechanism proposes that toxicity is associated with the hyperphosphorylated form of tau. Alternatively, in a loss of function mechanism, precipitation of tau could cause the unbound microtubules in the neuron to become destabilized and to depolymerize, resulting in a loss of neuronal structural integrity.

Tau is an intrinsically unstructured protein consisting of 441 amino acids (longest isoform) and lacking well-defined globular domains (*4*). The natively disordered structure of tau has to date prevented high-resolution structure determination (*7*−*15*). Although tau contains no globular domains, a number of functional domains have been identified (Figure 1) (*16*). These domains include a proline-rich domain (PRD), three to four repeats of tubulin-binding domains (TBDs) separated by short linker regions, and two hydrophobic domains (A and B) (*17*−*20*). The hydrophobic domains and the TBDs are critical for both microtubule binding and NFT formation. In addition, over 30 phosphorylation sites in tau have been identified. The phosphorylation sites are concentrated within two regions: the proline-rich domain, which links the hydrophobic domains and the TBDs, and the extreme *C*-terminus, which is associated with caspase cleavage (*4*). The observation of hyperphosphorylation in the proline-rich domain of tau suggests that the proline-rich domain may be important to phosphorylation-induced conformational change.

The type II polyproline helix (PPII) is a common secondary structure, which is often observed in proline-rich sequences (*21*, *22*). PPII is a relatively extended conformation ($\phi = -75°$, $\psi = +145°$) and is an important conformation in protein−protein interfaces (*23*, *24*). Propensity scales for PPII formation indicate that both serine and threonine have very low PPII propensities; interestingly, both residues are also quite common in proline-rich regions (*25*−*30*). We hypothesized that changes in hydrogen-bonding capabilities and side chain-backbone (*31*, *32*) interactions due to phosphorylation might increase the PPII propensities of serine and threonine, leading to a conformational switch to PPII

† This work was supported by the University of Delaware Research Foundation, the American Heart Association, and the University of Delaware. Support for undergraduate research to A.A.B. was provided by the Howard Hughes Medical Institute and the Barry M. Goldwater Foundation.

* To whom correspondence should be addressed. Tel: +1-302-831-0197. Fax: +1-302-831-6335. E-mail: zondlo@udel.edu.

[1] Abbreviations: AD, Alzheimer's disease; CD, circular dichroism; DIPEA, diisopropylethylamine; DMF, *N*,*N*-dimethylformamide; HPLC, high performance liquid chromatography; HSQC, heteronuclear single quantum coherence; $^1J_{H\alpha C\alpha}$, 1-bond coupling constant between the alpha proton and the alpha carbon; $^3J_{\alpha N}$, 3-bond coupling constant between the alpha proton and the amide proton; MAP, microtubule-associated protein; NFT, neurofibrillary tangle; NMR, nuclear magnetic resonance; PPII, left-handed type II polyproline helix; PRD, proline-rich domain; TFA, trifluoroacetic acid; TOCSY, total correlation spectroscopy; t_R, retention time by HPLC.; TSP, 3-trimethylsilylpropionate.

10.1021/bi052662c CCC: $33.50
Published on Web 04/05/2006

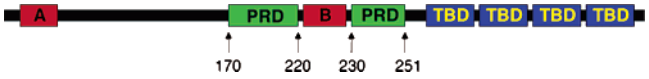

FIGURE 1: Schematic representation of the largest isoform of tau (441 residues). A and B (red) indicate hydrophobic regions of tau that contribute to microtubule binding. PRD (green) indicates the proline-rich domain of tau. TBD indicates the tubulin-binding domains.

upon phosphorylation. This hypothesis is supported by the observation that proteins containing phosphorylated serine or phosphorylated threonine are observed to bind to proteins as ligands in a PPII conformation (*33*−*36*). The WW domain of Pin1, a prolyl isomerase important in Alzheimer's disease, binds phosphorylated tau but not nonphosphorylated tau in a PPII conformation (*33*, *37*−*42*). The binding of Pin1 and other proteins to phosphorylated proteins in a PPII conformation suggests a phosphorylatation-induced switch to PPII as a potentially important conformational change in proteins.

Although tubulin-binding-domain (TBD) repeats are required for microtubule binding, the TBD repeats alone bind microtubules with lower affinity without an *N*-terminal or *C*-terminal extension. Weak microtubule binding also may occur without TBDs as long as both the *N*-terminal and the *C*-terminal extensions are present (*17*−*20*). Current models of the interactions between microtubules and tau assign the *N*-terminal A and B domains as hydrophobic regions that provide additional binding energy to the tau−microtubule complex. The proline-rich domain is thought to support microtubule binding, in conjunction with the TBDs and a *C*-terminal extension. Under a global hairpin structural model of tau and the jaws microtubule-binding model proposed by Mandelkow, structural changes in the proline-rich regions could have a major effect on microtubule binding affinity (*15*, *16*, *18*, *43*). In particular, a conformational switch to PPII has the potential to cause large-scale structural changes within the protein because PPII is a relatively rigid and extended structure compared to the random coil.

The mechanisms by which tau hyperphosphorylation may cause microtubule dissociation and aggregation are still poorly understood. To understand phosphorylation-induced conformational changes in tau, peptides derived from the proline-rich region were examined in their phosphorylated and nonphosphorylated states using circular dichroism (CD) and NMR spectroscopy (*37*, *43*−*48*).

EXPERIMENTAL SECTION

Peptide Synthesis and Characterization. Peptides were synthesized via standard Fmoc solid-phase peptide synthesis using Rink amide resin (0.1 or 0.25 mmol) on a Rainin PS3 peptide synthesizer. The resin was swelled in DMF for 5 min prior to the start of the synthesis. Amino acid couplings were performed using Fmoc amino acids (4 equiv) and HBTU (4 equiv). The following steps were used for peptide synthesis per cycle: (1) removal of the Fmoc group with 20% piperidine in DMF, 3 × 5 min; (2) resin wash (DMF, 5 × 1 min); (3) amide coupling (amino acid, HBTU, and 0.05 M DIPEA in DMF; 20 min for the first eight amino acids and 50 min for the remaining amino acids); and (4) rinse (DMF, 3 × 1 min). Trityl-protected serine and threonine were incorporated at phosphorylation sites to allow for selective phosphorylation. After the addition of the final residue, the peptide was deprotected (20% piperidine in DMF, 3 × 5 min) and the amino terminus acetylated (10% acetic anhydride in pyridine, 5 min). The resin was washed with DMF (6×) and CH_2Cl_2 (3×).

Nonphosphorylated peptides were cleaved and deprotected in a trifluoroacetic acid (TFA)/thioanisole/ethanedithiol/phenol/water (84:4:4:4:4) cocktail for 2−4 h. The peptides were concentrated under nitrogen and precipitated with ether. The precipitate was dissolved in water, and the resulting solution was filtered and purified by reverse phase HPLC (Vydac semipreparative C18, 10 × 250 mm, 5 μm particle size, 300 Å pore). The peptides were purified using gradients of buffer B (80% MeCN, 20% H_2O, and 0.05% TFA) in buffer A (98% H_2O, 2% MeCN, and 0.06% TFA) as indicated below. The peptides were purified to homogeneity, as indicated by the presence of a single peak upon reinjection on analytical HPLC (Microsorb MV C18, 4.6 × 250 mm, 100 Å pore). Phosphorylated peptides were synthesized by chemical phosphorylation on resin by the following procedure: (1) The trityl group was deprotected with 2% TFA, 5% triethylsilane (TES), and 93% CH_2Cl_2 (3 × 1 min, or until the flow-through solution was colorless). (2) Phosphitylation was performed under nitrogen by the addition of tetrazole (1.35 mmol; 3 mL of 3% tetrazole solution in MeCN (Transgenomics)) and *O*,*O*-dibenzyl-*N*,*N*-diisopropylphosphoramidite (500 μL, 1.52 mmol, Fluka) and allowed to react for 5−6 h with mixing. The solution was removed and the resin washed with DMF (3×) and CH_2Cl_2 (3×). This step was repeated for peptides with greater than 5 phosphorylation sites; (3) oxidation was performed with *tert*-butyl hydroperoxide (4 mL of a 3 M solution in CH_2Cl_2) and allowed to react with mixing for 1 h. The solution was removed and the resin washed with DMF (3×), MeOH (3×), and CH_2Cl_2 (3×). The phosphorylated peptides were purified and characterized as described previously for nonphosphorylated peptides.

Phosphorylated $tau_{174-183}$ was purified using a linear gradient of 0−15% buffer B (20% water, 80% acetonitrile, and 0.05% TFA) in buffer A (98% water, 2% acetonitrile, and 0.06% TFA) over 60 min. The peptides $tau_{174-183}$, phosphorylated $tau_{196-212}$, and phosphorylated $tau_{229-238}$ were purified using a linear gradient of 0−20% buffer B in buffer A over 60 min. The peptides $tau_{196-209}$, $tau_{229-238}$, $tau_{229-242}$, and phosphorylated $tau_{196-209}$ were purified using a linear gradient of 0−25% buffer B in buffer A over 60 min. The peptides $tau_{211-219}$ and phosphorylated $tau_{229-242}$ were purified using a linear gradient of 0−30% buffer B in buffer A over 60 min. The peptide $tau_{196-212}$ was purified using a linear gradient of 0−40% buffer B in buffer A over 60 min. Phosphorylated $tau_{211-219}$ and $tau_{174-183}Tle_2$ were purified using a linear gradient of 10−40% buffer B in buffer A over 60 min.

Peptide identity was characterized by ESI-MS (positive ion mode, unless stated otherwise) on an LCQ Advantage (Finnigan) mass spectrometer. Analytical data for the peptides: $tau_{174-183}$ (t_R = 49.2 min, mass expected (exp.) 1073.6, mass observed (obs.) 1096.9 $(M + Na)^+$); $tau_{196-209}$ (t_R 41.1 min, exp. 1346.6, obs. 1346.9); $tau_{196-212}$ (t_R 30.2 min, exp. 1690.8, obs. 1691.8 $(M + H)^+$); $tau_{211-219}$ (t_R 56.4 min, exp. 1168.6, obs. 1169.8 $(M + H)^+$); $tau_{229-238}$ (t_R 40.0 min, exp. 1258.7, obs. 1259.7 $(M + H)^+$); $tau_{229-242}$ (t_R 41.7 min, exp. 1700.9, obs. 851.8 $(M + H)^{2+}$); phosphorylated $tau_{174-183}$ (t_R 39.7 min, exp. 1232.6, obs. 1256.5 $(M + Na)^+$);

Table 1: Summary of CD Data for Tau Peptides[a]

peptide	Θ_{228} (deg cm^2 dmol^{-1})	λ at local Θ_{max} (nm)	local Θ_{max} (deg cm^2 dmol^{-1})	λ at Θ_{min} (nm)	Θ_{min} (deg cm^2 dmol^{-1})
$tau_{174-183}$	−510	n.a.[b]	n.a.	202	−8660
phosphorylated $tau_{174-183}$	270	226	280	202	−13300
$tau_{174-183}Tle_2$	−1620	n.a.	n.a.	203	−11300
$tau_{196-209}$	−2450	213	−4620	195	−10200
phosphorylated $tau_{196-209}$	−2360	n.a.	n.a.	198	−14000
$tau_{196-212}$	−1910	215	−3190	196	−9540
phosphorylated $tau_{196-212}$	−1310	n.a.	n.a.	197	−14200
$tau_{211-219}$	−740	231	−590	201	−17000
phosphorylated $tau_{211-219}$	250	229	320	201	−18000
$tau_{229-238}$	−1170	n.a.	n.a.	201	−21400
phosphorylated $tau_{229-238}$	780	228	780	200	−28000
$tau_{229-238}$, pH 7.2	−800	n.a.	n.a.	201	−20400
phosphorylated $tau_{229-238}$, pH 7.2	530	228	530	200	28300
$tau_{229-238}$, pH 6.5	−1060	n.a.	n.a.	201	−21300
phosphorylated $tau_{229-238}$, pH 6.5	−460	229	−340	200	−30100
$tau_{229-238}$, D_2O	−800	n.a.	n.a.	200	−21100
phosphorylated $tau_{229-238}$, D_2O	1060	228	1060	199	−28200
$tau_{229-242}$	−1540	n.a.	n.a.	201	−22100
phosphorylated $tau_{229-242}$	−470	230	−460	199	−23200

[a] CD data were collected with 150 μM peptide in 5 mM potassium phosphate (pH 8.0) and 25 mM KF. [b] No local maxima were observed.

phosphorylated $tau_{196-209}$ (t_R 22.2 min, exp. 1746.7, obs. 872.5 $(M - 2H)^{2-}$ (negative ion mode)); phosphorylated $tau_{196-212}$ (t_R 22.5 min, exp. 2250.6, obs. 1124.6 $(M - 2H)^{2-}$ (negative ion mode)); phosphorylated $tau_{211-219}$ (t_R 27.8 min, exp. 1408.6, obs 705.6 $(M + 2H)^{2+}$); phosphorylated $tau_{229-238}$ (t_R 39.9 min, exp. 1498.7, obs. 750.0 $(M + 2H)^{2+}$); phosphorylated $tau_{229-242}$ (t_R 37.3 min, exp. 2020.9, obs. 1011.8 $(M + 2H)^{2+}$); $tau_{174-183}Tle_2$ (t_R 39.5 min, exp. 1097.9, obs 1098.7 $(M+H)^+$).

Circular Dichroism. Circular dichroism (CD) spectra were collected at 25 °C on a Jasco J-810 spectropolarimeter in a 1 mm cell. Standard CD solutions were made with 5 mM phosphate buffer (pH 8.0), 25 mM KF, and 150 μM peptide. The peptide concentration was determined by UV−vis based on tyrosine absorbance ($\epsilon = 1280$ M^{-1} cm^{-1} at 280 nm in water) on a Perkin-Elmer Lambda 25 spectrometer for all peptides except $tau_{174-183}$. Initial concentrations of $tau_{174-183}$ and phosphorylated $tau_{174-183}$ were determined by peptide absorbance using the equation: $(\mu g/mL) = (A_{215} - A_{225}) \times 144$ (*49*, *50*). Final concentrations of $tau_{174-183}$ and phosphorylated $tau_{174-183}$ were determined, after the completion of the CD experiments, by the addition of 150 μM benzaldehyde to the solutions used for the CD experiments and integration by NMR. The spectra represent the average of at least three independent trials taken with scans made at 1 nm intervals with 4 s signal integration time and 1 nm bandwidth. Data were background-corrected but were not smoothed. Local maxima reported in Table 1 were calculated from smoothed data. Error bars indicate standard error.

$tau_{174-183}$ $K_{174}TPPAPKTPP_{183}$

$tau_{196-209}$ $G_{196}YSSPGSPGTPGSR_{209}$

$tau_{196-212}$ $G_{196}YSSPGSPGTPGSRSRT_{212}$

$tau_{211-219}$ $YR_{211}TPSLPTPP_{219}$

$tau_{229-238}$ $YV_{229}RTPPKSPSS_{238}$

$tau_{229-242}$ $V_{229}RTPPKSPSSAKSR_{242}Y$

FIGURE 2: Sequences of peptides examined in this study. The residue numbers indicated are from the largest tau isoform. The residues in green indicate sites of phosphorylation. All peptides were acetylated on the *N*-terminus and contained *C*-terminal amides.

NMR Spectroscopy. Peptides were dissolved in buffer containing 5 mM potassium phosphate (pH 6.5), 25 mM NaCl, 90% H_2O/10% D_2O, and 100 μM TSP. Peptide concentrations were 200 μM−1 mM. NMR spectra were recorded at 296 K on a Brüker AVC 600 MHz NMR spectrometer with a triple-resonance cryoprobe. 1-D NMR spectra were recorded using a gradient watergate pulse sequence and a 2−3 s relaxation delay. Watergate TOCSY spectra were recorded for all peptides for resonance assignment. $^3J_{\alpha N}$ was determined directly from the 1-D spectra. Errors in $^3J_{\alpha N}$ are estimated to be ≤0.2 Hz. The value of ϕ was calculated on the basis of the parametrized Karplus equation, $^3J_{\alpha N} = 6.51 \cos^2(\phi - 60) - 1.76 \cos(\phi - 60) + 1.6$ (*51*).

^{1}H-^{13}C HSQC spectra were recorded for both the nonphosphorylated and the phosphorylated variants of the peptides $tau_{174-183}$ and $tau_{229-238}$. The peptides were dissolved in buffer containing 5 mM potassium phosphate (pH 8.0), 25 mM NaCl, 100% D_2O, and 100 μM TSP. Peptide concentrations were 500 μM−2 mM. NMR spectra were recorded at 296 K. Watergate TOCSY spectra were recorded to confirm resonance assignments. Spectra were recorded with and without ^{13}C-decoupling using spectral widths of 9 and 130 ppm. $^1J_{H\alpha C\alpha}$ coupling constants were measured directly from the HSQC spectra recorded without decoupling and were confirmed by comparison with the differences in chemical shift for the resonance recorded with decoupling. Errors in $^1J_{H\alpha C\alpha}$ are estimated to be ±0.5 Hz. The value of ψ was calculated on basis of the measured $^1J_{H\alpha C\alpha}$, with the values of ϕ determined directly from $^3J_{\alpha N}$ and the parametrized Karplus equation, $^1J_{H\alpha C\alpha} = 140.3 + 1.4 \sin(\psi+138) - 4.1 \cos(2(\psi + 138)) + 2.0 \cos(2(\phi + 30))$ (*52*). Notably, this Karplus equation exhibits a local maximum at $\psi = +132°$, a value that is nearly ideal for a canonical polyproline helix; therefore, if $^1J_{H\alpha C\alpha}$ is near this local maximum, then two reasonable solutions to ψ are expected.

RESULTS

A series of tau-derived peptides was synthesized to determine the conformational effects of the hyperphosphorylation of tau. Peptide sequences were chosen to include sequences in tau that were both proline-rich and contained multiple phosphorylation sites (Figure 2). The phosphorylation sites in the peptides were chosen on the basis of those residues identified as phosphorylated in the diseased state (*4*). All phosphorylated peptides were synthesized by chemical phosphorylation and purified to homogeneity by HPLC,

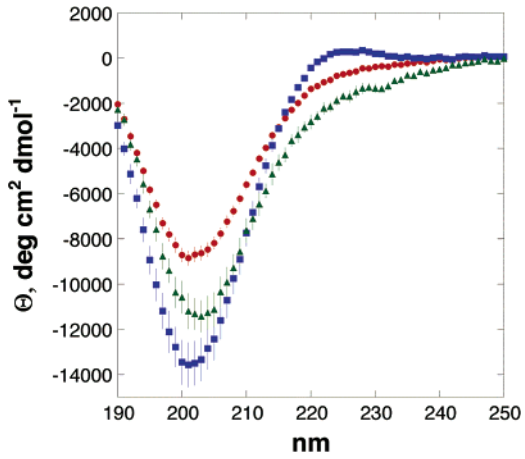

FIGURE 3: CD spectra of nonphosphorylated tau$_{174-183}$ (red circles), phosphorylated tau$_{174-183}$ (blue squares), and the negative control tau$_{174-183}$Tle$_2$ (green triangles). Phosphorylation induced a change favoring PPII structure as indicated by the induction of a positive band at 228 nm in phosphorylated tau$_{174-183}$, characteristic of PPII.

ensuring that each experiment was conducted with the peptide fully phosphorylated site-specifically at the residues indicated.

In peptides lacking a naturally occurring tyrosine residue, a tyrosine residue was incorporated at the *N*-terminus or *C*-terminus for concentration determination. The site of tyrosine incorporation was chosen to avoid cis−trans isomerization induced by Tyr-Pro or Pro-Tyr sequences (*53*). Tau$_{174-183}$ did not include a tyrosine because it was observed that either an *N*-terminal or *C*-terminal tyrosine induced local structural changes in the peptide (results not shown).

Tau$_{174-183}$. Phosphorylated and nonphosphorylated tau$_{174-183}$ were examined using circular dichroism (CD) spectroscopy to determine the conformational effects of phosphorylation. A comparison of the CD spectra of the nonphosphorylated and phosphorylated peptides revealed a significant conformational difference between the two peptides (Figure 3 and Table 1). The phosphorylation of tau$_{174-183}$ induced a conformational change favoring type II polyproline helix (PPII). PPII has a characteristic CD spectrum with a maximum at 228 nm. Phosphorylation favored the PPII conformation, as seen by the increase in mean residue ellipticity at 228 nm (Θ_{228}) for the phosphorylated versus the nonphosphorylated peptide. As a negative control, the peptide tau$_{174-183}$Tle$_2$ was synthesized, which contains the sterically congested *tert*-leucine residue in place of both Thr residues. Sterically congested β-branched amino acids strongly disfavor PPII (*25*, *26*, *28*−*30*). Tau$_{174-183}$Tle$_2$ exhibited a significantly reduced Θ_{228}, indicating a loss of PPII compared to either nonphosphorylated tau$_{174-183}$ or phosphorylated tau$_{174-183}$.

NMR spectroscopy revealed that phosphorylated tau$_{174-183}$ adopted a polyproline helix conformation. Characteristic ϕ and ψ dihedral angles for PPII are −75° and +145°, respectively. Near-ideal values of ϕ and ψ were observed in phosphorylated tau$_{174-183}$. (Table 2) (*54*). In addition, phosphorylated tau$_{174-183}$ exhibited a significant increase in amide chemical shift dispersion (from 0.30 (nonphoshorylated) to 0.79 ppm (phosphorylated) (data not shown); phosphothreonine δ = 9.09 and 8.96 ppm compared to threonine δ = 8.29 and 8.22 ppm). The most dramatic change in the NMR data was a significant reduction in the Thr $^3J_{\alpha N}$ coupling constants (3.3 and 4.4 Hz in phosphorylated tau$_{174-183}$ versus 7.3 and 7.3 Hz in nonphosphorylated tau$_{174-183}$; the *tert*-leucine $^3J_{\alpha N}$ coupling constants were 8.1 and 8.4 Hz in the disrupted PPII control peptide tau$_{174-183}$Tle$_2$) (*55*−*57*). These results indicate that phosphorylation induces significant ordering of the peptide, particularly at the phosphothreonine residues.

Table 2: NMR-Derived Data for Nonphosphorylated and Phosphorylated Tau$_{174-183}$[a]

	nonphosphorylated		phosphorylated			
residue	$^3J_{\alpha N}$	ϕ	$^3J_{\alpha N}$	ϕ	$^1J_{H\alpha C\alpha}$	ψ[b]
Lys	7.0	−82	7.0	−82	n.d.	n.d.
Lys	7.0	−82	7.0	−82	141.8	115, 152
Ala	5.5	−71	5.5	−71	143.3	128, 136
Thr	7.3	−84	3.3	−54	143.4	111, 153
Thr	7.3	−84	4.4	−63	142.6	112, 155
Pro[c]	n.a.	−60 ± 25	n.a.	−60 ± 25	147.8	[d]
Pro[c]	n.a.	−60 ± 25	n.a.	−60 ± 25	148.5	[d]

[a] The residues were not assigned site-specifically because of sequence redundancy. Coupling constants are measured in Hz; n.a. indicates not applicable and n.d. indicates not determined because of spectral overlap. [b] Values of ψ shown represent the two solutions near the local maximum at ψ = +132° in the Karplus equation (*52*). [c] Only 2 proline resonances were well-resolved in the ^{1}H-^{13}C HSQC experiment. [d] A parametrized Karplus equation relating ψ and $^1J_{H\alpha C\alpha}$ for Pro residues has not been reported.

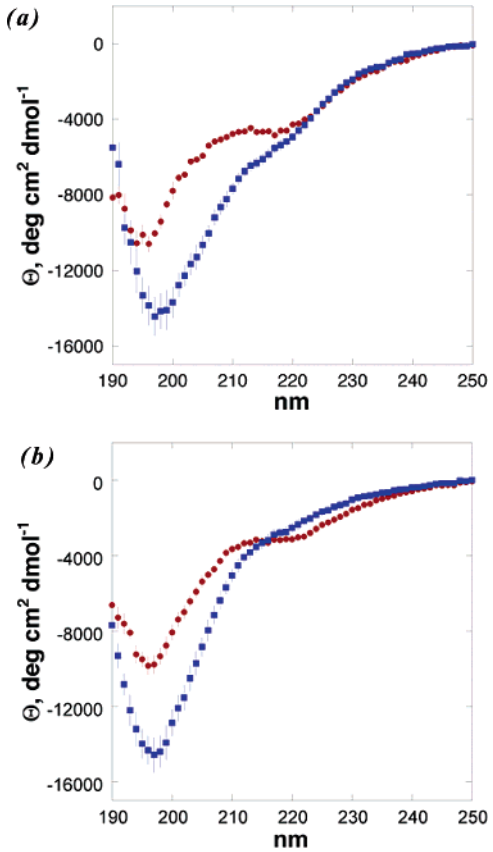

FIGURE 4: (a) CD spectra of nonphosphorylated tau$_{196-209}$ (red circles) and phosphorylated tau$_{196-209}$ (blue squares). (b) CD spectra of nonphosphorylated tau$_{196-212}$ (red circles) and phosphorylated tau$_{196-212}$ (blue squares).

Tau$_{196-209}$ *and Tau*$_{196-212}$. Comparison of the CD spectra of phosphorylated and nonphosphorylated tau$_{196-209}$ indicates a large phosphorylation-induced change (Figure 4a and Table 1). The CD spectrum of nonphosphorylated tau$_{196-209}$ showed

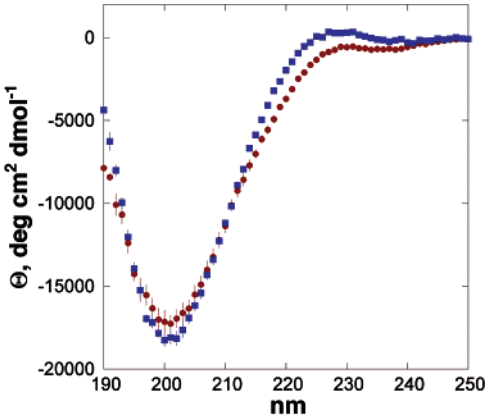

FIGURE 5: CD spectra of nonphosphorylated $tau_{211-219}$ (red circles) vs phosphorylated $tau_{211-219}$ (blue squares). Phosphorylation induced a conformational change favoring PPII structure as indicated by the increase in Θ_{228} of phosphorylated $tau_{211-219}$.

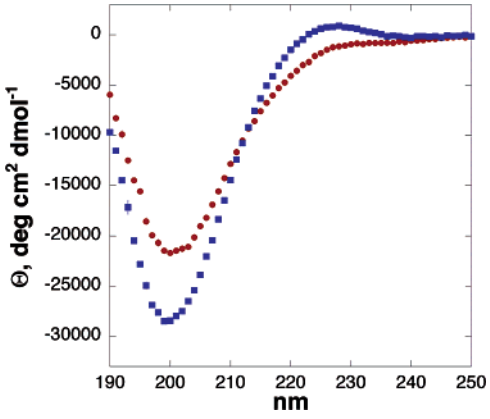

FIGURE 6: CD spectra of nonphosphorylated $tau_{229-238}$ (red circles) and phosphorylated $tau_{229-238}$ (blue squares). Phosphorylation induced a conformational change favoring PPII, indicated by the increase in Θ_{228} of phosphorylated $tau_{229-238}$.

a well-defined local minimum at 216 nm and a local maximum at 213 nm, reminiscent of denatured α-helical structure. Phosphorylated $tau_{196-209}$ lacked the local minima and maxima observed in the nonphosphorylated peptide, indicating that phosphorylation disrupted the nascent α-helix (*58*, *59*). In addition, phosphorylated $tau_{196-209}$ exhibited an increase in the magnitude of the mean residue ellipticity at the minimum at 197 nm.

An extension of $tau_{196-209}$, $tau_{196-212}$, included three additional residues and two additional phosphorylation sites. As expected, the conformational changes observed between the nonphosphorylated and phosphorylated versions of $tau_{196-212}$ were similar to conformational changes observed in $tau_{196-209}$ (Figure 4b and Table 1). The nonphosphorylated peptide had a local minimum at 220 nm and a local maximum at 215 nm. Phosphorylation eliminated these local minima and maxima and resulted in an increase in Θ at 228 nm and a decrease at 197 nm.

$Tau_{211-219}$. A comparison of the CD spectra of nonphosphorylated and phosphorylated $tau_{211-219}$ revealed a significant conformational change (Figure 5 and Table 1). Nonphosphorylated $tau_{211-219}$ showed weak residual PPII character. Phosphorylation induced a conformational change that further favored the PPII secondary structure, with an increase in the Θ_{228} from −730 deg cm^2 dmol^{-1} in the nonphosphorylated peptide to 290 deg cm^2 dmol^{-1} upon phosphorylation. As was observed in $tau_{174-183}$, phosphorylation induced significant ordering in the threonine residues (phosphothreonine $^3J_{\alpha N} = 3.1$ and 5.5 Hz for phosphorylated $tau_{211-219}$ compared to threonine $^3J_{\alpha N} = 6.2$ and 7.0 Hz for nonphosphorylated $tau_{211-219}$).

$Tau_{229-238}$ and $Tau_{229-242}$. CD spectra of nonphosphorylated and phosphorylated $tau_{229-238}$ showed a considerable phosphorylation-induced conformational change favoring PPII (Figure 6 and Table 1). The Θ_{228} value increased from −1150 deg cm^2 dmol^{-1} in nonphosphorylated $tau_{229-238}$ to 900 deg cm^2 dmol^{-1} in the phosphorylated peptide. These experiments were conducted at pH 8.0, ensuring the dianionic form of the phosphate group. CD experiments on $tau_{229-238}$ were also performed at pH 6.5 and pH 7.2 to identify whether a conformational change was induced simply by the presence of a phosphate group, or if the conformational change was dependent on the charge state. As expected, nonphosphorylated $tau_{229-238}$ had identical CD spectra at pH 6.5, pH 7.2, and pH 8.0 (results not shown). All experimental conditions indicated a phosphorylation-induced conformational change favoring PPII. Phosphorylated $tau_{229-238}$ showed a much larger conformational change at pH 8.0 and pH 7.2, where the phosphate is predominantly in the dianionic form, than at pH 6.5, where the phosphate is predominantly in the monoanionic form (Figure 7 and Table 1). These results indicate an electronic component to the phosphorylation-induced conformational change, as has been observed previously for phosphorylated peptides. CD experiments were also performed in D_2O at pH 8.0. These experiments were used to address possible D_2O-induced increases in PPII, as a control for HSQC experiments (see below) (*60*). In D_2O, only very minor increases in Θ_{228} were observed in both the phosphorylated and nonphosphorylated $tau_{229-238}$ peptides compared to the results in H_2O (Table 1).

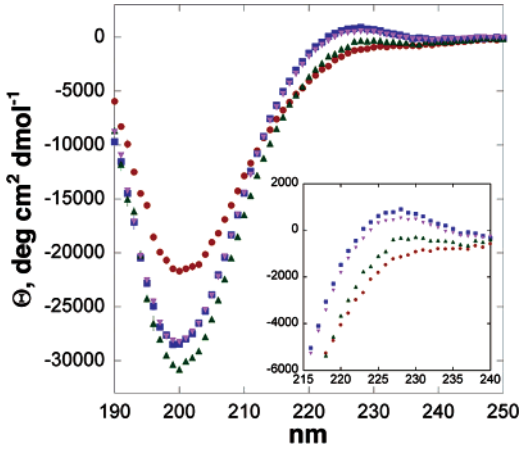

FIGURE 7: CD spectra of phosphorylated $tau_{229-238}$ at pH 6.5 (green triangles), phosphorylated $tau_{229-238}$ at pH 7.2 (purple reverse triangles), phosphorylated $tau_{229-238}$ at pH 8.0 (blue squares), and nonphosphorylated $tau_{229-238}$ (red circles). The CD spectra of nonphosphorylated $tau_{229-238}$ at pH 6.5 and pH 8.0 are identical (Table 1).

NMR indicated that phosphorylated $tau_{229-238}$ adopted a polyproline helix conformation, with coupling constant data indicating near-ideal values of ϕ and ψ (Table 3). Phosphorylation also significantly increased the amide chemical shift dispersion (data not shown; 0.95 ppm dispersion for phosphorylated $tau_{229-238}$ versus 0.40 ppm for nonphosphorylated $tau_{229-238}$; phosphoserine (8.74 and 9.96 ppm) and phosphothreonine (8.80 ppm) residues were also significantly down-

Table 3: NMR-Derived Data for Phosphorylated $Tau_{229-238}$[a]

residue	$^3J_{\alpha N}$	ϕ	$^1J_{H\alpha C\alpha}$	ψ[b]
Val229	8.8	−98	142.0	132
Arg230	6.6	−79	141.7	111, 153
pThr231	4.8	−65	141.7	101, 162
Pro[c]	n.a.	−60 ± 25	149.3	[d]
Pro[c]	n.a.	−60 ± 25	148.4	[d]
Lys234	6.6	−79	142.5	124, 140
pSer[c]	5.5	−71	n.d.	n.d.
Pro[c]	n.a.	−60 ± 25	148.1	[d]
pSer[c]	6.2	−76	142.5	117, 147
Ser238	5.9	−74	141.8	108, 156

[a] Resonances in the nonphosphorylated peptide showed very poor chemical shift dispersion precluding analysis. Coupling constants are measured in Hz; n.a. indicates not applicable and n.d. indicates not determined because of spectral overlap. [b] Values of ψ shown represent the two solutions near the local maximum at $\psi = +132°$ in the Karplus equation (*52*). [c] Phosphoserine and proline residues were not assigned site-specifically. [d] A parametrized Karplus equation relating ψ and $^1J_{H\alpha C\alpha}$ for Pro residues has not been reported.

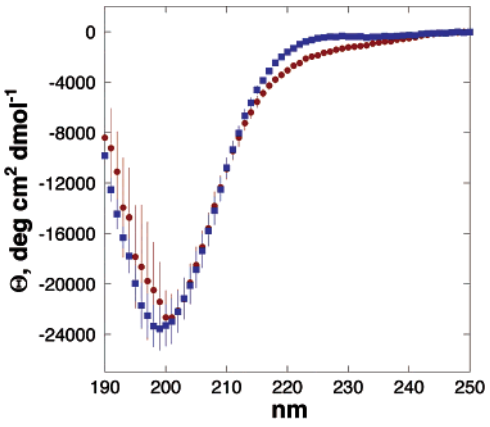

FIGURE 8: CD spectra of nonphosphorylated $tau_{229-242}$ (red circles) and phosphorylated $tau_{229-242}$ (blue squares). Phosphorylation induced a conformational change favoring PPII, indicated by an increase in Θ_{228} of phosphorylated $tau_{229-242}$.

field-shifted compared to the nonphosphorylated variants (8.23−8.40 ppm)). As was observed with $tau_{174-183}$ and $tau_{211-219}$, phosphoserine and phosphothreonine exhibited restricted values of $^3J_{\alpha N}$ (phosphothreonine 4.8 Hz; phosphoserine 5.5 and 6.2 Hz).

$Tau_{229-242}$, a four residue *C*-terminal extension of $tau_{229-238}$, included one additional phosphorylation site. The conformational change between the phosphorylated and nonphosphorylated $tau_{229-242}$ was similar to the change in the $tau_{229-238}$ peptides, although the magnitude of the change in mean residue ellipticity was smaller in $tau_{229-242}$ owing to the larger number of residues (Figure 8). Reduced PPII character in both the phosphorylated and nonphosphorylated peptides, compared to that of the $tau_{229-238}$ peptides, indicates that the additional four *C*-terminal residues do not strongly support PPII.

DISCUSSION

$Tau_{174-183}$. Phosphorylation of $tau_{174-183}$ induced a conformational change favoring PPII conformation. The conformational change was similar to that expected if the threonine residues, which have a low PPII propensity, were replaced with Glu residues, which have a high PPII propensity. The NMR data, in particular, indicated conformational restriction at the phosphothreonine residue compared to the usually larger observed coupling constants for Thr residues. The magnitude of the conformational change, as observed both by NMR and by CD, was particularly noteworthy, considering that $tau_{174-183}$ only contained two phosphorylation sites. A common feature observed in $tau_{174-183}$ and other tau peptides that demonstrated a strong induction of PPII upon phosphorylation was the presence of a positively charged amino acid prior to the phosphorylated residue. In $tau_{174-183}$, each threonine was preceded by a lysine residue and followed by two prolines. This context may be an indicator for significant phosphorylation-induced conformational changes favoring PPII.

$Tau_{196-209}$ and $Tau_{196-212}$. Although the phosphorylation-induced conformational changes in $tau_{196-209}$ and $tau_{196-212}$ could not be definitively characterized, phosphorylation caused a distinct disruption of local structure. The local minima and maxima in these peptides, which are suggestive of a denatured α-helix, were significantly reduced in $tau_{196-209}$ and eliminated in $tau_{196-212}$ upon phosphorylation. Phosphorylation has been observed to reduce α-helix stability in the absence of specific stabilizing interactions such as favorable helix−dipole interactions (*55*, *56*, *58*, *59*, *61*−*66*). Unlike the other tau peptides studied herein, phosphorylation of $tau_{196-209}$ and $tau_{196-212}$ did not induce a well-defined PPII conformation. It is expected that phosphorylation will induce a polyproline helix only in sequences with a high propensity for PPII. The lack of an observed increase in PPII in $tau_{196-209}$ and $tau_{196-212}$ is likely due to the large number of glycine residues, which are conformationaly flexible and are generally unfavorable for PPII. $Tau_{196-212}$, a three-residue *C*-terminal extension of $tau_{196-209}$, incorporated two additional phosphorylation sites. As expected, $tau_{196-212}$ showed a greater conformational change and disruption of local structure than $tau_{196-209}$ because of these additional phosphorylation sites.

$Tau_{211-219}$. Nonphosphorylated $tau_{211-219}$ showed weak residual PPII character. This residual PPII conformation was not surprising, considering that this short 10-residue peptide contained four prolines. The PPII character in the peptide significantly increased upon phosphorylation. As in $tau_{174-183}$, one of the threonines was preceded by a positively charged amino acid (arginine). Again, the presence of a preceding basic residue may be an indicator for significant phosphorylation-induced conformational changes favoring PPII.

$Tau_{229-238}$ and $Tau_{229-242}$. Phosphorylation of $tau_{229-238}$ induced a large conformational change favoring a PPII conformation, as indicated by CD and NMR. This region corresponds to a known recognition sequence of the WW domain of Pin1, which binds proteins in a PPII conformation. Pin1, a prolyl cis−trans isomerase, binds its targets only upon phosphorylation with a greater than 3.0 kcal mol^{-1} preference for the phosphorylated over nonphosphorylated ligands (*33*). Pin1 is a critical protein important in Alzheimer's disease, with loss of Pin1 activity associated with increased neuronal cell death. Retention of Pin1 activity in neuronal cells decreases neurofibrillary tangle formation and restores the function of tau via the interaction of Pin1 with tau (*38*, *41*, *42*). Our results indicate that the phosphorylation of the Pin1 recognition site induces a conformational change favoring PPII, preorganizing the phosphorylated peptide for recognition by the Pin1 WW domain.

$Tau_{229-242}$ showed similar phophorylation-induced conformational changes as that in $tau_{229-238}$ but in a larger peptide context. The four-residue *C*-terminal extension was found to decrease average PPII content in both the phosphorylated and the nonphosphorylated peptides. These results are not surprising because the extension only contains one phosphorylation site and does not contain any proline residues.

Conformational Effects of Protein Phosphorylation. Phosphorylation induced a conformational change in each of the tau peptides examined. A common feature of the conformational change induced by phosphorylation was an induction of PPII structure. Not surprisingly, the magnitude of the change in conformation favoring PPII varied among the peptides depending on the sequence. Specifically, induction of PPII depended significantly on the identity of the adjacent amino acids that could directly interact with the phosphate group. A common motif found in peptides that strongly favored PPII upon phosphorylation was a positively charged amino acid preceding the phosphorylation site. Notably, all peptides showing significant induction of PPII upon phosphorylation contained other strongly PPII-favoring residues (Pro, Lys, Ala, and Arg) in the sequences. Further experiments are necessary to determine the specific interactions of the phosphate group with neighboring amino acids and the conditions that cause phosphorylation to induce a conformational change to PPII. However, the data herein indicate that phosphorylation in proline-rich regions may be a general mechanism to induce a conformational switch to a more ordered PPII structure.

Notably, all phosphothreonine residues exhibited small $^3J_{\alpha N}$ coupling constants (3.1−5.5 Hz; mean = 4.2 Hz) indicative of conformationally restricted ϕ. In addition, the phosphorylated residues exhibited significantly downfield-shifted amide chemical shifts. The observation of phosphoserine conformational restriction has been previously observed in model peptides, where it was ascribed to hydrogen bond formation between the phosphate and the backbone amide protons of the phosphoserine and/or the two preceding residues (*55*−*57*, *63*, *67*). Downfield-shifted phosphoserine and/or phosphothreonine amide chemical shifts have also been ascribed to phosphate-backbone amide hydrogen bonds (*48*). Current data are insufficient to assign the observed changes to specific hydrogen bonding interactions; additional experiments to understand the specific forces stabilizing PPII for phosphorylated peptides are necessary.

Previous analyses of phosphorylation-dependent structure in nonglobular regions of proteins have revealed evidence for significant conformational changes dependent on phosphorylation (*43*, *47*, *48*, *55*−*59*, *61*−*63*, *65*−*80*). These conformational changes have been frequently characterized as an order-to-disorder transition, with the unfolding of α-helices being a commonly observed effect of protein phosphorylation (*79*, *81*). Stabilization of α-helices upon phosphorylation has also been observed in numerous cases, indicating a context dependence for the conformational effects of phosphorylation (*59*, *61*, *62*, *64*−*66*). Within proline-rich sequences, phosphorylyation has been observed to induce conformational changes consistent with adopting PPII, although these changes have not in general been interpreted as such (*43*, *69*, *72*). The small magnitude of the positive band associated with PPII, as well as the similarities of the CD spectra of PPII and random coil, makes the assignment of PPII particularly challenging in larger peptides and proteins (*82*).

Table 4: Crystallographic Data on Phosphoserine/Phosphothreonine-Containing Ligands in Protein−Protein Complexes

binding domain	protein	pdb code	phosphorylated residue in ligand	ϕ	ψ	ref
Polo-box domain	Polo-like kinase	1UMW	phosphoThr	−63	+126	*35*
BRCT domain	BRCA	1T29	phosphoSer	−65	+126	*36*
WW domain	Pin1	1F8A	phosphoSer	−62	+148	*33*
FHA domain	Rad53	1G6G	phosphoThr	−68	+145	*34*

Interestingly, the conformational change to PPII induced by phosphorylation was, in certain cases, as large as the change to PPII caused by replacing serine or threonine, which are unfavorable residues for PPII, with glutamic acid, which is a favorable residue for PPII. Glu is commonly used as a mimic of phosphoserine or phosphothreonine because of similar steric and electrostatic properties (*44*, *45*, *83*−*87*). The data herein suggest that mimicry of phosphoserine or phosphothreonine with Glu may also approximate the conformational effects of phosphorylation.

In protein−protein complexes, phosphoserine- and phosphothreonine-containing ligands are commonly observed bound in a polyproline helix conformation. Crystal structures of the ligands of the Pin1 WW domain, the BRCT domain of BRCA, the FHA domain of Rad53, and the Polo box domain of Polo-like kinase, all indicate that the phosphorylated ligand is bound in a PPII conformation (Table 4) (*33*−*36*). The structure of the ligand of the FHA domain of Rad53 is particularly intriguing because PPII is observed over a sequence of 6 nonproline residues. In combination with the crystallographic data, the data herein suggest that PPII may be a preferred conformation for binding phosphoserine- or phosphothreonine-containing ligands because of the different conformational preferences of the phosphorylated versus the nonphosphorylated serine or threonine residues. Binding nonphosphorylated serine- or threonine-containing ligands in a PPII conformation is energetically unfavorable because of a required conformational change. In contrast, PPII may be a preferred conformation of phosphoserine and phosphothreonine. Therefore, binding phosphorylated proteins in a PPII conformation results in increased specificity for the phosphorylated over the nonphosphorylated ligands.

Induction of PPII structure in the proline-rich region may have broader structural and functional implications for tau. PPII is an ordered and relatively extended conformation with a 3.1 Å rise per residue, as compared to 1.5 Å rise per residue in an α-helix. Tau is natively disordered and has a flexible structure. Thus, the induction of an extended and ordered structure to a previously flexible region within the protein may induce long-range structural changes in the protein (Figure 9; see refs *16*, *18*, and *43* for other models that are also consistent with the data herein). The proline-rich region is an important linker region in microtubule binding: Mandelkow has proposed a jaws binding model for microtubule binding in which the proline-rich region is a linker between the tubulin-binding domains and the hydrophobic A and B domains. The hydrophobic domains act synergistically with the tubulin-binding domains to bind tightly to microtubules

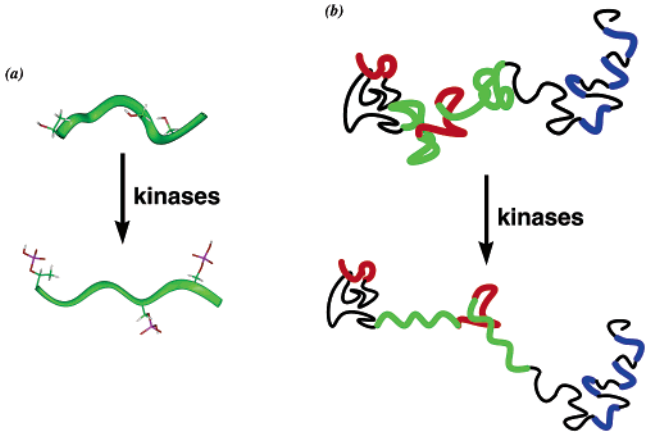

FIGURE 9: One model of the (a) local and (b) global effects of a phosphorylation-induced conformational change on tau structure.

(*16*, *18*, *20*, *88*). Moreover, nonphosphorylated tau adopts a global hairpin structure in which the *N*-terminus, *C*-terminus, and tubulin-binding domains are close in space (*15*). A change in structure of the proline-rich domain to a more ordered and extended conformation has the potential to change the relative distances and orientations of these hydrophobic domains, possibly disrupting the hairpin fold and reducing microtubule binding affinity, thereby exposing the hydrophobic residues of tau.

Cis−trans isomerization in hyperphosphorylated tau is critical to its formation of paired helical fragments, neurofibrillary tangles, and pathogenesis. The loss of activity of Pin1, a prolyl cis−trans isomerase, results in increased neurofibrillary tangle formation and neuronal cell death, whereas the retention of Pin1 activity prevents the aggregation of hyperphosphorylated tau and restores microtubule-binding activity (*38*, *41*, *42*). Previous studies with peptides have shown that phosphorylation does not inherently change the cis−trans isomerization equilibrium. Similar (and very low) populations of the cis isomer were observed in the nonphosphorylated and phosphorylated states of the peptides, including tau-derived peptides, as was also observed here (*33*, *43*, *70*, *89*−*91*). Therefore, phosphorylation-induced changes in the cis−trans isomerization state, as observed in hyperphosphorylated tau, are not primarily due to local sequence effects. Instead, the observed changes in cis−trans isomerization depend primarily on long-range interactions induced by phosphorylation. We propose phosphorylation-induced conformational changes to a polyproline helix in the proline-rich domains as one possible trigger to generate the long-range interactions that are necessary to induce cis−trans isomerization.

Aberrant misfolding and aggregation of tau is a central element of a number of neurodegenerative disorders collectively termed tauopathies (*92*−*94*). These tauopathies are also often characterized by phosphorylation-dependent changes in tau. More generally, numerous microtubule-associated proteins exhibit activities that are controlled by phosphorylation within proline-rich sequences (*95*−*97*). The data herein suggest a general role of phosphorylation-dependent conformational changes in tauopathies and in the structures and functions of microtubule-associated proteins.

The results herein have broad implications for the conformational effects of protein phosphorylation. Phosphorylation by kinases represents the most common posttranslational modification (*98*). Moreover, proline-rich domains are among the most common domains in eukaryotes (*99*). The phosphorylation of serine and threonine residues within proline-rich sequences may provide a general mechanism for kinase-controlled conformational changes to a polyproline helix conformation in proteins.

CONCLUSIONS

We have examined the local conformational effects of the hyperphosphorylation of peptides derived from the proline-rich domain of tau via NMR and circular dichroism. The data indicate that phosphorylation of proline-rich regions of tau induces conformational changes to polyproline helix. Significant conformational changes were localized to the phosphorylated residues. These data suggest that phosphorylation-mediated conformational changes to polyproline helix may be involved in the global structural and functional transformation of tau from its less-phosphorylated microtubule-bound form to the hyperphosphorylated, aggregated form. More generally, the data herein suggest that phosphorylation may be a general mechanism to induce conformational changes in the proline-rich regions of proteins to the polyproline helix conformation.

ACKNOWLEDGMENT

We thank Krista Thomas, Alaina Brown, and Shalini Balakrishnan for preliminary experiments.

REFERENCES

1. Lee, V. M. Y., Balin, B. J., Otvos, L., and Trojanowski, J. Q. (1991) A68 - a major subunit of paired helical fragments and derivatized forms of normal tau, *Science 251*, 675−678.
2. Goedert, M., Spillantini, M. G., Cairns, N. J., and Crowther, R. A. (1992) Tau-proteins of Alzheimer's paired helical filaments - abnormal phosphorylation of all 6 brain isoforms, *Neuron 8*, 159−168.
3. Bramblett, G. T., Goedert, M., Jakes, R., Merrick, S. E., Trojanowski, J. Q., and Lee, V. M. Y. (1993) Abnormal tau-phosphorylation at Ser(396) in Alzheimers-disease recapitulates development and contributes to reduced microtubule-binding, *Neuron 10*, 1089−1099.
4. Buée, L., Bussière, T., Buée-Scherrer, V., Delacourte, A., and Hof, P. R. (2000) Tau protein isoforms, phosphorylation and role in neurodegerative disorders, *Brain Res. Rev. 33*, 95−130.
5. Shahani, N., and Brandt, R. (2002) Functions and malfunctions of the tau proteins, *Cell. Mol. Life Sci. 59*, 1668−1680.
6. Avila, J., Lucas, J. J., Pérez, M., and Hernández, F. (2004) Role of tau protein in both physiological and pathological conditions, *Physiol. Rev. 84*, 361−384.
7. Lippens, G., Wieruszeski, J.-M., Leroy, A., Smet, C., Sillen, A., Buée, L., and Landrieu, I. (2004) Proline-directed random-coil chemical shift values as a tool for the NMR assignment of the tau phosphorylation sites, *ChemBioChem 5*, 73−78.
8. Smet, C., Leroy, A., Sillen, A., Wieruszeski, J.-M., Landrieu, I., and Lippens, G. (2004) Accepting its random coil nature allows a partial NMR assignment of the neuronal tau protein, *ChemBioChem 5*, 1639−1646.
9. Sillen, A., Leroy, A., Wieruszeski, J.-M., Loyens, A., Beauvillain, C., Buée, L., Landrieu, I., and Lippens, G. (2005) Regions of tau implicated in the paired helical fragment core as defined by NMR, *ChemBioChem 6*, 1849−1856.
10. Wright, P. E., and Dyson, H. J. (1999) Intrinsically unstructured proteins: re-assessing the protein structure-function paradigm, *J. Mol. Biol. 293*, 321−331.
11. Dunker, A. K., Brown, C. J., Lawson, J. D., Iakoucheva, L. M., and Obradovic, Z. (2002) Intrinsic disorder and protein function, *Biochemistry 41*, 6573−6582.
12. Eliezer, D., Barré, P., Kobaslija, M., Chan, D., Li, X., and Heend, L. (2005) Residual structure in the repeat domain of tau: echoes

of microtubule binding and paired helical filament formation, *Biochemistry 44*, 1026−1036.
13. Oldfield, C. J., Ulrich, E. L., Cheng, Y. G., Dunker, A. K., and Markley, J. L. (2005) Addressing the intrinsic disorder bottleneck in structural proteomics, *Proteins: Struct., Funct., Bioinf. 59*, 444−453.
14. Mukrasch, M. D., Biernat, J., von Bergen, M., Griesinger, C., Mandelkow, E., and Zweckstetter, M. (2005) Sites of tau important for aggregation populate β-structure and bind to microtubules and polyanions, *J. Biol. Chem. 280*, 24978−24986.
15. Jeganathan, S., von Bergen, M., Brutlach, H., Steinhoff, H.-J., and Mandelkow, E. (2006) Global hairpin folding of tau in solution, *Biochemistry 45*, 2283−2293.
16. Gamblin, T. C. (2005) Potential structure/function relationships of predicted secondary structural elements of tau, *Biochim. Biophys. Acta 1739*, 140−149.
17. Brandt, R., and Lee, G. (1993) Functional-organization of microtubule-associated protein−tau−identification of regions which affect microtubule growth, nucleation, and bundle formation in vitro, *J. Biol. Chem. 268*, 3414−3419.
18. Gustke, N., Trinczek, B., Biernat, J., Mandelkow, E. M., and Mandelkow, E. (1994) Domains of tau-protein and interactions with microtubules, *Biochemistry 33*, 9511−9522.
19. Trinczek, B., Biernat, J., Baumann, K., Mandelkow, E. M., and Mandelkow, E. (1995) Domains of tau-protein, differential phosphorylation, and dynamic instability of microtubules, *Mol. Biol. Cell. 6*, 1887−1902.
20. Goode, B. L., Denis, P. E., Panda, D., Radeke, M. J., Miller, H. P., Wilson, L., and Feinstein, S. C. (1997) Functional interactions between the proline-rich and repeat regions of tau enhance microtubule binding and assembly, *Mol. Biol. Cell 8*, 353−365.
21. Adzhubei, A. A., and Sternberg, M. J. E. (1993) Left-handed polyproline-II helices commonly occur in globular-proteins, *J. Mol. Biol. 229*, 472−493.
22. Williamson, M. P. (1994) The structure and function of proline-rich regions in proteins, *Biochem. J. 297*, 249−260.
23. Kay, B. K., Williamson, M. P., and Sudol, P. (2000) The importance of being proline: the interaction of proline-rich motifs in signaling proteins with their cognate domains, *FASEB J. 14*, 231−241.
24. Zarrinpar, A., Bhattacharyya, R. P., and Lim, W. A. (2003) The structure and function of proline recognition domains, *Sci. STKE 2003*, re8.
25. Kelly, M. A., Chellgren, B. W., Rucker, A. L., Troutman, J. M., Fried, M. G., Miller, A. F., and Creamer, T. P. (2001) Host−guest study of left-handed polyproline II helix formation, *Biochemistry 40*, 14376−14383.
26. Rucker, A. L., Pager, C. T., Campbell, M. N., Qualls, J. E., and Creamer, T. P. (2003) Host−guest scale of left-handed polyproline II helix formation, *Proteins 53*, 68−75.
27. Fitzkee, N. C., and Rose, G. D. (2004) Reassessing random-coil statistics in unfolded proteins, *Proc. Natl. Acad. Sci. U.S.A. 101*, 12497−12502.
28. Jha, A. K., Colubri, A., Zaman, M. H., Koide, S., Sosnick, T. R., and Freed, K. F. (2005) Helix, sheet, and polyproline II frequencies and strong nearest neighbor effects in a restricted coil library, *Biochemistry 44*, 9691−9702.
29. Shi, Z., Chen, K., Liu, Z., Ng, A., Bracken, W. C., and Kallenbach, N. R. (2005) Polyproline II propensities from GGXGG peptides reveal an anticorrelation with β-sheet scales, *Proc. Natl. Acad. Sci. U.S.A. 102*, 17964−17968.
30. Brown, A. M., and Zondlo, N. J. A Thermodynamic propensity scale for type II polyproline helices, submitted for publication.
31. Bretscher, L. E., Jenkins, C. L., Taylor, K. M., DeRider, M. L., and Raines, R. T. (2001) Conformational stability of collagen relies on a stereoelectronic effect, *J. Am. Chem. Soc. 123*, 777−778.
32. Hinderaker, M. P., and Raines, R. T. (2003) An electronic effect on protein structure, *Protein Sci. 12*, 1188−1194.
33. Verdecia, M. A., Bowman, M. E., Lu, K. P., Hunter, T., and Noel, J. P. (2000) Structural basis for phosphoserine-proline recognition by group IV WW domains, *Nat. Struct. Biol. 7*, 639−643.
34. Durocher, D., Taylor, I. A., Sarbassova, D., Haire, L. F., Westcott, S. L., Jackson, S. P., Smerdon, S. J., and Yaffe, M. B. (2000) The molecular basis of FHA domain: phosphopeptide binding specificity and implications for phospho-dependent signaling mechanisms, *Mol. Cell 6*, 1169−1182.
35. Elia, A. E. H., Rellos, P., Haire, L. F., Chao, J. W., Ivins, F. J., Hoepker, K., Mohammad, D., Cantley, L. C., Smerdon, S. J., and Yaffe, M. B. (2003) The molecular basis for phosphodependent substrate targeting and regulation of Plks by the Polo-box domain, *Cell 115*, 83−95.
36. Clapperton, J. A., Manke, I. A., Lowery, D. M., Ho, T., Haire, L. F., Yaffe, M. B., and Smerdon, S. J. (2004) Structure and mechanism of BRCA1 BRCT domain recognition of phosphorylated BACH1 with implications for cancer, *Nat. Struct. Mol. Biol. 11*, 512−518.
37. Wintjens, R., Wieruszeski, J.-M., Drobecq, H., Rousselot-Pailley, P., Buée, L., Lippens, G., and Landrieu, I. (2001) ^{1}H NMR study on the binding of Pin1 Trp-Trp domain with phosphothreonine peptides, *J. Biol. Chem. 276*, 25150−25156.
38. Lu, P. J., Wulf, G., Zhou, X. Z., Davies, P., and Lu, K. P. (1999) The prolyl isomerase Pin1 restores the function of Alzheimer-associated phosphorylated tau protein, *Nature 399*, 784−788.
39. Lu, P. J., Zhou, X. Z., Shen, M. H., and Lu, K. P. (1999) Function of WW domains as phosphoserine- or phosphothreonine-binding modules, *Science 283*, 1325−1328.
40. Zhou, X. Z., Kops, O., Werner, A., Lu, P. J., Shen, M. H., Stoller, G., Kullertz, G., Stark, M., Fischer, G., and Lu, K. P. (2000) Pin1-dependent prolyl isomerization regulates dephosphorylation of Cdc25C and tau proteins, *Mol. Cell 6*, 873−883.
41. Liou, Y. C., Sun, A., Ryo, A., Zhou, X. Z., Yu, Z. X., Huang, H. K., Uchida, T., Bronson, R., Bing, G. Y., Li, X. J., Hunter, T., and Lu, K. P. (2003) Role of the prolyl isomerase Pin1 in protecting against age-dependent neurodegeneration, *Nature 424*, 556−561.
42. Lu, K. P., Liou, Y. C., and Vincent, I. (2003) Proline-directed phosphorylation and isomerization in mitotic regulation and in Alzheimer's disease, *Bioessays 25*, 174−181.
43. Daly, N. L., Hoffmann, R., Otvos L., Jr., and Craik, D. J. (2000) Role of phosphorylation in the conformation of tau peptides implicated in Alzheimer's disease, *Biochemistry 39*, 9039−9046.
44. Eidenmüller, J., Fath, T., Hellwig, A., Reedd, J., Sontag, E., and Brandt, R. (2000) Structural and functional implications of tau hyperphosphorylation: information from phosphorylation-mimicking mutated tau proteins, *Biochemistry 39*, 13166−13175.
45. Rankin, C. A., Sun, Q., and Gamblin, T. C. (2005) Pseudophosphorylation of tau at Ser202 and Thr205 affects tau filament formation, *Mol. Brain. Res. 138*, 84−93.
46. Necula, M., and Kuret, J. (2005) Site-specific pseudophosphorylation mudulates the rate of tau filament dissociation, *FEBS Lett. 579*, 1453−1457.
47. Du, J.-T., Li, Y.-M., Ma, Q.-F., Qiang, W., Zhao, Y.-F., Abe, H., Kanazawa, K., Qin, X.-R., Aoyagi, R., Ishizuka, Y., Nemeto, T., and Nakanishi, H. (2005) Synthesis and conformational properties of phosphopeptides related to the human tau protein, *Regul. Pept. 130*, 48−56.
48. Du, J.-T., Li, Y.-M., Wei, W., Wu, G.-S., Zhao, Y.-F., Kanazawa, K., Nemoto, T., and Nakanishi, H. (2005) Low-barrier hydrogen bond between phosphate and the amide group in phosphopeptide, *J. Am. Chem. Soc. 127*, 16350−16351.
49. Waddell, W. J. (1956) A simple ultraviolet spectrophotometric method for the determination of protein, *J. Lab. Clin. Med. 48*, 311−314.
50. (1986) *Practical Protein Chemistry: A Handbook* (Darbre, A., Ed.) Vol. 16, Wiley & Sons, New York.
51. Vuister, G. W., and Bax, A. (1993) Quantitative J correlation: a new approach for measuring homonuclear three-bond $J_{HNH\alpha}$ coupling constants in ^{15}N-enriched proteins, *J. Am. Chem. Soc. 115*, 7772−7777.
52. Vuister, G. W., Delaglio, F., and Bax, A. (1992) An empirical correlation between $^1J_{C\alpha H\alpha}$ and protein backbone conformation, *J. Am. Chem. Soc. 114*, 9674−9675.
53. Meng, H. Y., Thomas, K. M., Lee, A. E., and Zondlo, N. J. (2006) Effects of *i* and *i*+3 residue identity on cis−trans isomerism of the Aromatic$_{i+1}$-Prolyl$_{i+2}$ amide bond: implications for type VI beta-turn formation *Biopolymers (Peptide Sci.) 84*, 192−204.
54. Lam, S. L., and Hsu, V. L. (2003) NMR identification of left-handed polyproline type II helices, *Biopolymers 69*, 270−281.
55. Shen, T., Wong, C. F., and McCammon, J. A. (2001) Atomistic brownian dynamics simulation of peptide phosphorylation, *J. Am. Chem. Soc. 123*, 9107−9111.
56. Hamelberg, D., Shen, T., and McCammon, J. A. (2005) Phosphorylation effects on cis/trans isomerization and the backbone conformation of serine-proline motifs: accelerated molecular dynamics analysis, *J. Am. Chem. Soc. 127*, 1969−1974.
57. Wong, S. E., Bernacki, K., and Jacobson, M. (2005) Competition between intramolecular hydrogen bonds and solvation in phos-

phorylated peptides: simulations with explicit and implicit solvent, *J. Phys. Chem. B 109*, 5249−5258.
58. Szilak, L., Moitra, J., Krylov, D., and Vinson, C. (1997) Phosphorylation destabilizes α-helices, *Nat. Struct. Biol. 4*, 112−114.
59. Andrew, C. D., Warwicker, J., Jones, G. R., and Doig, A. J. (2002) Effect of phosphorylation on α-helix stability as a function of position, *Biochemistry 41*, 1897−1905.
60. Chellgren, B. W., and Creamer, T. P. (2004) Effects of H_2O and D_2O on polyproline II helical structure, *J. Am. Chem. Soc. 126*, 14734−14735.
61. Szilak, L., Moitra, J., and Vinson, C. (1997) Design of a leucine zipper coiled coil stabilized 1.4 kcal mol^{-1} by phosphorylation of a serine in the e position, *Protein Sci. 6*, 1273−1283.
62. Radhakrishnan, I., Pérez-Alvarado, G. C., Dyson, H. J., and Wright, P. E. (1998) Conformational preferences in Ser^{133}-phosphorylated and nonphosphorylated forms of the kinase inducible transactivation domain of CREB, *FEBS Lett. 430*, 317−322.
63. Ramelot, T. A., and Nicholson, L. K. (2001) Phosphorylation-induced structural changes in the amyloid precursor protein cytoplasmic tail detected by NMR, *J. Mol. Biol. 307*, 871−884.
64. Signarvic, R. S., and DeGrado, W. F. (2003) De Novo Design of a Molecular switch: phosphorylation-dependent association of designed peptides, *J. Mol. Biol. 334*, 1−12.
65. Errington, N., and Doig, A. J. (2005) A phosphoserine-lysine salt bridge with an α-helical peptide, the strongest α-helix side-chain interaction measured to date *Biochemistry 44*, 7553−7558.
66. Mendieta, J., Fuertes, M. A., Kunjishapatham, R., Santa-María, I., Moreno, F., Alonso, C., Gago, F., Muñoz, V., Avila, J., and Hernández, F. (2005) Phosphorylation modulates the alpha-helical structure and polymerization of a peptide from the third tau microtubule-binding repeat, *Biochim. Biophys. Acta 1721*, 16−26.
67. Tholey, A., Lindemann, A., Kinzel, V., and Reed, J. (1999) Direct effects of phosphorylation on the preferred backbone conformation of peptides: a nuclear magnetic resonance study, *Biophys. J. 76*, 76−87.
68. Wright, D. E., Noiman, E. S., Chock, P. B., and Chau, V. (1981) Fluorometric assay for adenosine 3′,5′-cyclic monophosphate-dependent protein-kinase and phosphoprotein phosphatase-activities, *Proc. Natl. Acad. Sci. U.S.A. 78*, 6048−6050.
69. Hollosi, M., Otvos, L., Urge, L., Kajtar, J., Perczel, A., Laczko, I., Vadasz, Z. S., and Fasman, G. D. (1993) Ca^{2+}-induced conformational transitions of phosphorylated peptides, *Biopolymers 33*, 497−510.
70. Schutkowski, M., Bernhardt, A., Zhou, X. Z., Shen, M. H., Reimer, U., Rahfeld, J. U., Lu, K. P., and Fischer, G. (1998) Role of phosphorylation in determining the backbone dynamics of the serine/threonine-proline motif and Pin1 substrate recognition, *Biochemistry 37*, 5566−5575.
71. Parker, D., Jhala, U. S., Radhakrishnan, I., Yaffe, M. B., Reyes, C., Shulman, A. I., Cantley, L. C., Wright, P. E., and Montminy, M. (1998) Analysis of an activator: coactivator complex reveals an essential role for secondary structure in transcriptional activation, *Mol. Cell 2*, 353−359.
72. Bienkiewicz, E. A., Moon Woody, A.-Y., and Woody, R. W. (2000) Conformation of the RNA polymerase II C-terminal domain: circular dichroism of long and short fragments, *J. Mol. Biol. 297*, 119−133.
73. Johnson, L. N., and Lewis, R. J. (2001) Structural basis for control by phosphorylation, *Chem. Rev. 101*, 2209−2242.
74. Kar, S., Sakaguchi, K., Shimohigashi, Y., Samaddar, S., Banerjee, R., Basu, G., Swaminathan, V., Kundu, T. K., and Roy, S. (2002) Effect of phosphorylation on the structure and fold of the transactivation domain of p53, *J. Biol. Chem. 277*, 15579−15585.
75. Stultz, C. M., Levin, A. D., and Edelman, E. R. (2002) Phosphorylation-induced conformational change in a mitogen-activated protein kinase substrate, *J. Biol. Chem. 277*, 47653−47661.
76. Penrose, K. J., Garcia-Alai, M., de Prat-Gay, G., and McBride, A. A. (2004) Casein kinase II phosphorylation-induced conformational switch triggers degradation of the papillomavirus E2 protein, *J. Biol. Chem. 279*, 22430−22439.
77. Arrigoni, G., Marin, O., Pagano, M. A., Settimo, L., Paolin, B., Meggio, F., and Pinna, L. A. (2004) Phosphorylation of calmodulin fragments by protein kinase CK2. Mechanistic aspects and structural consequences, *Biochemistry 43*, 12788−12798.
78. Obsilova, V., Herman, P., Vecer, J., Sulc, M., Teisinger, J., and Obsil, T. (2004) 14−3−3ζ C-terminal stretch changes its conformation upon ligand binding and phosphorylation at Thr232, *J. Biol. Chem. 279*, 4531−4540.
79. Metcalfe, E. E., Traaseth, N. J., and Veglia, G. (2005) Serine 16 phosphorylation induces an order-to-disorder transition in monomeric phospholamban, *Biochemistry 44*, 4386-4396.
80. Liu, L. L., and Franz, K. J. (2005) Phosphorylation of an α-synuclein fragment enhances metal binding, *J. Am. Chem. Soc. 127*, 9662−9663.
81. Iakoucheva, L. M., Radivojac, P., Brown, C. J., O'Connor, T. R., Sikes, J. G., Obradovic, Z., and Dunker, A. K. (2004) The importance of intrinsic disorder for protein phosphorylation, *Nucleic Acids Res. 32*, 1037−1049.
82. Shi, Z. S., Woody, R. W., and Kallenbach, N. R. (2002) Is polyproline II a major backbone conformation in unfolded proteins? *Adv. Protein Chem. 62*, 163−240.
83. Davis, B. G. (2004) Mimicking posttranslational modifications of proteins, *Science 303*, 480−482.
84. Huffine, M. E., and Scholtz, J. M. (1996) Energetic implications for protein phosphorylation: conformational stability of HPr variants that mimic phosphorylated forms, *J. Biol. Chem. 271*, 28898−28902.
85. Eidenmüller, J., Fath, T., Maas, T., Pool, M., Sontag, E., and Brandt, R. (2001) Phosphorylation-mimicking glutamate clusters in the proline-rich region are sufficient to simulate the functional deficiencies of hyperphosphorylated tau protein, *Biochem. J. 357*, 759−767.
86. Necula, M., and Kuret, J. (2004) Pseudophosphorylation and glycation of tau protein enhance but do not trigger fibrillization in vitro, *J. Biol. Chem. 279*, 49694−49703.
87. Balakrishnan, S., and Zondlo, N. J. (2006) Design of a protein kinase-inducible domain, *J. Am. Chem. Soc.*, in press.
88. Gamblin, T. C., Berry, R. W., and Binder, L. I. (2003) Tau polymerization: role of the amino terminus, *Biochemistry 42*, 2252−2257.
89. Dugave, C., and Demange, L. (2003) Cis-trans isomerization of organic molecules and biomolecules: implications and applications, *Chem. Rev. 103*, 2475−2532.
90. Weiwad, M., Werner, A., Rucknagel, P., Schierhorn, A., Kullertz, G., and Fischer, G. (2004) Catalysis of proline-directed protein phosphorylation by peptidyl-prolyl cis/trans isomerases, *J. Mol. Biol. 339*, 635−646.
91. Smet, C., Wieruszeski, J.-M., Buée, L., Landrieu, I., and Lippens, G. (2005) Regulation of Pin1 peptidyl-prolyl cis/trans isomerase activity by its WW binding module on a multi-phosphorylated peptide of tau protein, *FEBS Lett. 579*, 4159−4164.
92. Feinstein, S. C., and Wilson, L. (2005) Inability of tau to properly regulate neuronal microtubule dynamics: a loss-of-function mechanism by which tau might mediate neuronal cell death, *Biochim. Biophys. Acta 1739*, 268−279.
93. Kosik, K. S., and Shimura, H. (2005) Phosphorylated tau and the neurodegenerative foldopathies, *Biochim. Biophys. Acta 1739*, 298−310.
94. Brandt, R., Hundelt, M., and Shahani, N. (2005) Tau alteration and neuronal degeneration in tauopathies: mechanisms and models, *Biochim. Biophys. Acta 1739*, 331−354.
95. Tokuraka, K., Katsuki, M., Nakagawa, H., and Kotani, S. (1999) A new model for microtunule-associated protein (MAP)-induced microtubule assembly, *Eur. J. Biochem. 259*, 158−166.
96. Sanchez Martin, C., Ledesma, D., Dotti, C. G., and Avila, J. (2000) Microtubule-associated protein-2 located in growth regions of rat hippocampal neurons is highly phosphorylated at its proline-rich region, *Neuroscience 101*, 885−893.
97. Sánchez, C., Díaz-Nido, J., and Avila, J. (2000) Phosphorylation of microtubule-associated protein 2 (MAP2) and its relevance for the regulation of the neuronal cytoskeleton function, *Prog. Neurobiol. 61*, 133−168.
98. Manning, G., Whyte, D. B., Martinez, R., Hunter, T., and Sudarsanam, S. (2002) The protein kinase complement of the human genome, *Science 298*, 1912−1934.
99. Rubin, G. M., Yandell, M. D., W. J., Miklos, G. L. G., Nelson, C. R., Hariharan, I. K., Fortini, M. E., Li, P. W., Apweiler, R., Fleischmann, W., Cherry, J. M., Henikoff, S., Skupski, M. P., Misra, S., Ashburner, M., Birney, E., Boguski, M. S., Brody, T., Brokstein, P., Celniker, S. E., Chervitz, S. A., Coates, D., Cravchik, A., Gabrielian, A., Galle, R. F., Gelbart, W. M., George, R. A., Goldstein, L. S. B., Gong, F. C., Guan, P., Harris, N. L., Hay, B. A., Hoskins, R. A., Li, J. Y., Li, Z. Y., Hynes, R. O.,

Jones, S. J. M., Kuehl, P. M., Lemaitre, B., Littleton, J. T., Morrison, D. K., Mungall, C., O'Farrell, P. H., Pickeral, O. K., Shue, C., Vosshall, L. B., Zhang, J., Zhao, Q., Zheng, X. Q. H., Zhong, F., Zhong, W. Y., Gibbs, R., Venter, J. C., Adams, M. D., and Lewis, S. (2000) Comparative genomics of the eukaryotes, *Science 287*, 2204−2215.

BI052662C